

HIGH POWER MICROSTRIP RF SWITCHES*

Soon D. Choi
James F. Boreham

Jet Propulsion Laboratory
California Institute of Technology
Pasadena, California

Abstract

A microstrip-type SPDT switch, using only two PIN diodes and eliminating usual dc blocking capacitors, has demonstrated an RF power handling capacity greater than 100 W CW at S-band. The insertion loss is less than 0.25 dB and the input-to-off port isolation is greater than 36 dB over a bandwidth larger than 30 MHz.

Introduction

Although coaxial-type solid-state RF switches have been previously reported, they were not suited for high power space applications.^{1, 2} The PIN diodes used in these switches had inadequate power-handling capability and the coaxial switch circuits were subjected to ionization breakdown at a relatively low power level. Recently, microstrip-compatible diodes with 1000 V reverse breakdown capability have become available. The microstrip-type solid-state diode switch reported here is superior to switch types currently used, such as the circulator and electromechanical types, in such aspects as power drain, weight, volume, magnetic cleanliness, cost, and reliability.

The basic concept of a diode switch is to transmit or reflect the RF power on a transmission line by means of altering the impedance states of one or more solid-state diodes. There are basically two switch types. In one type diodes are placed in shunt across the transmission line, while the other employs series diodes. Schematic drawings for the ON and OFF modes of the two switch types are shown in Fig. 1. For simplicity, the forward-biased switching element is represented with a short circuit and the reverse-biased element with an open circuit.

As is intuitively clear from the figure, the switching element in the series type should be able to handle the entire RF load power through the diode, whereas in shunt type, the switching element experiences a fraction of the total power because the shunt stub serves as a transformer parallel to the main line. Although the series type is inherently wide band, the shunt type is usually superior to the series type in several important aspects of switch characteristics, such as insertion loss, input-to-off port isolation, and power-handling capability.

In the shunt-type switch described in this article, a stub containing a switching diode is placed across a microstrip transmission line. When the switching diode is biased one way, the stub impedance at the main line is high and the RF power is unimpeded. Reversing the direction of the diode bias, the transmission line becomes shorted by a very low impedance presented by the stub. The number of the shunting stubs required in each arm of a switch is dictated primarily by the degree of isolation desired between the input and off port. The length and characteristic impedance of the stub are selected to yield optimum performance of the switch for a given set of diode parameters.

Presentation of the theoretical and measured result is preceded by brief characterization of the switching element and the microstrip substrate.

PIN Diode and Microstrip Substrate

Electrical equivalent circuits and typical parameters for the PIN diode used are shown in Fig. 2 and Table 1, respectively.

Table 1. Typical PIN diode parameters at 2295 MHz

Series resistance R_s	0.6 Ω	At +100 mA
Series inductance L_s	1.2 nH	(lead inductance)
Equivalent series resistance R_{sv}	1.8 Ω	At -200 V
Diode capacitance C_d	0.6 pF	At -200 V

The microstrip circuits are fabricated on 1.27-mm (0.050-in.) thick 99.5% pure alumina substrates with 0.05- μ m surface finish on the circuit side and 0.25- μ m finish on the ground plane side. Thickness of the gold metallization is 7.62- μ m. Relative permittivity and loss tangent of 99.5% pure alumina at 10 GHz are 9.7 and 0.0001, respectively.

Stub Design

Schematic diagrams of two shunt stub switches are shown in Fig. 3. Figure 3a shows a conventional microstrip switch configuration² in which a dc blocking capacitor is used. In this configuration one end of the diode is RF and dc grounded, which is usually accomplished by drilling a hole through the substrate for a ground post. The dc blocking capacitor is chosen so that, together with its series inductance, it is self-resonant at the band center frequency.

Figure 3b shows a new switch configuration which does not require the dc blocking capacitor or a ground post for the diode. Elimination of one capacitor and one ground post per stub could amount to considerable improvement in reliability and ease of manufacturing for multipole switches.

The stub impedance seen by the main line, Z_{in} , is given by $Z_{in} =$

$$\frac{(Z_3 \cos \phi_2 \cos \phi_3 - Z_2 \sin \phi_2 \sin \phi_3) + j(Z_d \cos \phi_2 \sin \phi_3)}{Z_2 (-Z_d \sin \phi_2 \sin \phi_3) + j(Z_2 \cos \phi_2 \sin \phi_3 + Z_3 \sin \phi_2 \cos \phi_3)} \quad (1)$$

*This paper presents the results of one phase of research carried out at the Jet Propulsion Laboratory, California Institute of Technology, under Contract No. NAS 7-100, sponsored by the National Aeronautics and Space Administration.

where

$$\phi_2 = \frac{2\pi}{\lambda_g} l_2$$

$$\phi_3 = \frac{2\pi}{\lambda_g} l_3$$

It is important in a switch that the maximum and minimum stub impedances should occur at the band center frequency f_0 so that the minimum insertion loss and the maximum isolation occur at this frequency.

Solving Eq. (1) for the stub lengths for a diode whose parameters are given in Table 1 yields

$$\left[l_2, l_3 \right] = \left[0.66 \left(\frac{\lambda_g 0}{4} \right), 1.15 \left(\frac{\lambda_g 0}{4} \right) \right] \quad (2)$$

or

$$\left[l_2, l_3 \right] = \left[0.34 \left(\frac{\lambda_g 0}{4} \right), 1.59 \left(\frac{\lambda_g 0}{4} \right) \right]$$

for $Z_2 = Z_3 = 50 \Omega$. It is clear that the lengths of the stub segments are quite different from a quarter wavelength. This is because of the complex nature of Eq. (1).³ The first set of the stub segments in Eq. (2) gives a shorter total length and it becomes for $\lambda_g 0/4 = 1.27 \text{ cm}$ ($f_0 = 2295 \text{ MHz}$), $[l_2, l_3] = [0.84 \text{ cm}, 1.46 \text{ cm}]$. Stubs are designed according to this formula and adjusted to yield the desired condition. The measured lengths were $[l_2, l_3] = [0.83 \text{ cm}, 1.46 \text{ cm}]$, which are in good agreement with the theoretical values.

Single-Pole Double-Throw Switch

A single-pole double throw (SPDT) switch can be formed by combining two single-pole single-throw (SPST) switches. The bias arrangement should be, of course, such that when one port is on, the other port is off. A photograph of a breadboard version of an SPDT switch is shown in Fig. 4. The insertion loss and the isolation for the SPDT switch are given, respectively, by

$$L_{\text{ins}} = 20 \log \left| 1 + \frac{Z_0}{2Z_{\text{in(ON)}}} + \frac{Z_{\text{in(OFF)}}}{2Z_0} \right| \quad (3)$$

$$L_{\text{iso}} = 20 \log \left| \frac{3}{2} + \frac{Z_0}{Z_{\text{in(OFF)}}} \right| \quad (4)$$

where $Z_{\text{in(ON)}}$ and $Z_{\text{in(OFF)}}$ are the stub impedances for switch on and off, respectively.

The measured data is plotted along with the theoretical curves given by Eqs. (3) and (4) in Fig. 5. The insertion loss at the band center frequency was 0.25 dB, which is the sum of losses due to launchers and main line (0.15 dB) and stub (0.04 dB) and the mismatch loss of the stub (0.06 dB). The measured data deviates from the theoretical curve less than 0.1 dB at 100 MHz away from the band center frequency. This discrepancy is believed to be due to neglecting the band limiting effect of the bias networks in the theoretical calculations. The measured data for the isolation agrees very well with the theoretical calculation.

Power and Vacuum Test

The SPDT switch shown in Fig. 4 was subjected to an ambient pressure power test. The input power was raised in increments of 25 W up to a maximum of 100 W. The switch was allowed sufficient time to

thermally stabilize at each power level. The temperature rise of the diode junction was 75 °C above the ambient temperature at the 100 W level. The power dissipated in the diode under this condition was calculated to be only 1.2 W.

The thermal resistance can be lowered by mounting the substrate on a solid metallic circuit frame and by using beryllium oxide dielectric directly beneath the diode.

The SPDT switch was also subjected to low pressure tests. When operated at critical pressure [306.6 N/m² (2.3 torr)], ionization breakdown did not occur until the input RF power reached 150 W. Additional tests were performed at $533.3 \times 10^{-5} \text{ N/m}^2$ ($4 \times 10^{-5} \text{ torr}$) to determine if multipacting breakdown would occur. None was observed for RF power levels as high as 150 W.

Applications

The theory developed here can be easily adapted for the design of switches for many different applications. A few of the switch types which could be used for switching between antennas and redundant receivers and transmitters was illustrated in Fig. 6, along with the matrices for the modes of operation and bias conditions. For the sake of simplicity, the stubs and diode bias networks are represented by diodes only.

These switches are combinations of SPST and SPDT switches. Therefore, the work presented in this report is the basic building block for many different switch types.

A transfer switch has been fabricated on a 2" × 3" × 0.050" substrate. Its characteristics are almost identical with those of the SPDT switch described here.

Conclusions

Extremely simple RF switches have been developed for applications in spacecraft radio systems. These switches use no other components but one PIN diode in each arm on microstrip substrates. A single-pole double-throw (SPDT) switch fabricated on a 2" × 2" × 0.05" or a transfer switch fabricated on a 2" × 3" × 0.05" alumina substrate can easily handle as much as 100 W of CW power at S-band. The insertion loss and isolation are better than 0.25 and 36 dB, respectively, over a 30 MHz band. The input VSWR is lower than 1.07 over the same bandwidth. These microstrip-type diode switches are superior to the currently used circulator and mechanical switches in terms of reliability, magnetic cleanliness, weight, volume, and power drain.

Acknowledgement

The authors wish to express their appreciation to John H. Meysenburg for his contribution to this work.

References

1. White, J. F., and Mortenson, K. E., "Diode SPDT Switching at High Power with Octave Microwave Bandwidth," *IEEE Trans. Microwave Theory and Techniques*, Vol. MTT-16, pp. 30-36, January 1968.
2. Watson, H. A., *Microwave Semiconductor Devices and Their Circuit Applications*, pp. 300-338. McGraw-Hill Book Co., Inc., New York, 1969.
3. Choi, S. D., "High-Power Microstrip RF Switch," *Quarterly Technical Review*, Vol. 1, No. 3, pp. 110-124, Oct. 1971, Jet Propulsion Laboratory, Pasadena, California.

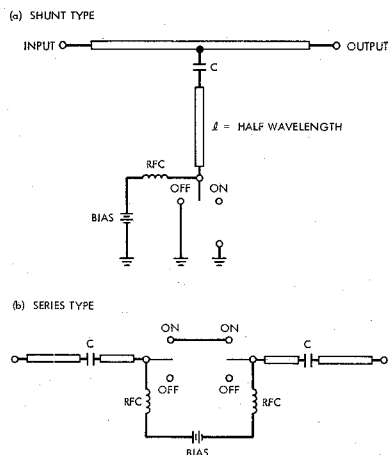


FIG. 1. SWITCH TYPES

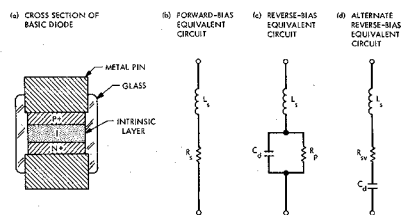


FIG. 2. EQUIVALENT CIRCUIT FOR PIN DIODES

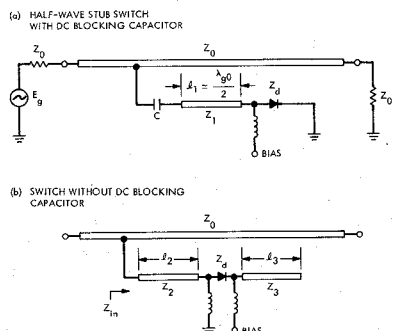


FIG. 3. SCHEMATIC DIAGRAM OF THE SHUNT STUB SPST SWITCHES

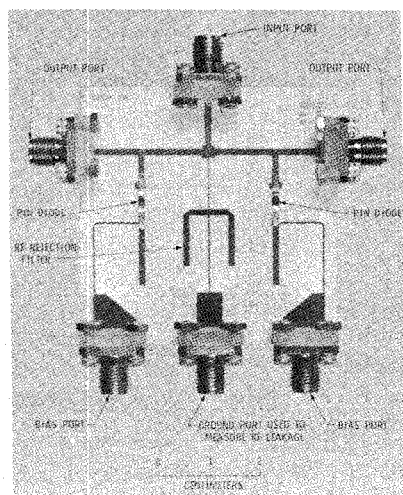


FIG. 4. BREADBOARD SPDT SWITCH

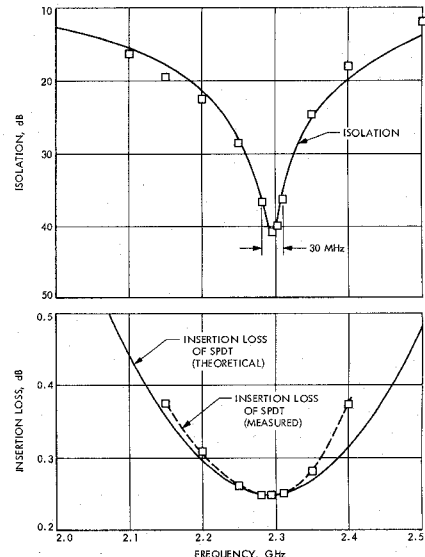


FIG. 5. INSERTION LOSS AND ISOLATION OF SPDT QUARTER-WAVE STUB SWITCH

SWITCH TYPE	SCHEMATIC DIAGRAM	MODE OF OPERATION	
		DIODE STATE [*]	DIODE STATE [*]
SPST		1-2 ON	F
		1-2 OFF	R
SPDT		1-2 ON	F
		1-3 OFF	R
		1-2 OFF	F
		1-3 ON	F
SPDT		1-2 ON	F R R
		1-3 ON	R F R
		1-4 ON	R R F F
2P2T		1-3 ON	F R F R
		1-4 ON	F R R F
		2-3 ON	R F F R
		2-4 ON	R R F R
TRANSFER		1-3 ON	R F R F
		2-4 ON	F R F R
		1-4 ON	F R F R
		2-3 ON	R F R F

^{*}DIODE STATES ASSUME QUARTER-WAVE STUBS. F AND R DESIGNATE FORWARD AND REVERSE BIASES, RESPECTIVELY.

FIG. 6. APPLICATION OF SPST AND SPDT SWITCHES TO FORM OTHER SWITCH TYPES